

USING THE FINITE - TIME DISTURBANCE OBSERVER (FTO) FOR ROBOTIC MANIPULATOR ALMEGA 16

DÙNG BỘ QUAN SÁT NHIỄU VỚI THỜI GIAN HỮU HẠN CHO TAY MÁY ROBOT ALMEGA 16

Vo Thu Ha

ABSTRACT

This paper presents build a finite time observator (FTO) and applies it to the Almega16 robot motion system. The main content of the article is to design a FTO so that the observation of the external noise of the Almega16 robot motion system will converge to the desired true value over a period of time. finite, is done by estimating the external noise quantities and then feeding them into the available Robot controller. The advantage when applying the FTO disturbance monitor is that it is possible to eliminate the inverse inertia matrix component in the dynamic equation. The results achieved showed that the Almega16 robot movement system ensures that the errors of the rotating joints quickly reach zero with a small transition time, making the closed system stable according to Lyapunov standards.

Keywords: Robot Almega 16, Finite - time observer, Lyapunov standards.

TÓM TẮT

Bài báo trình bày xây dựng bộ quan sát nhiễu với thời gian hữu hạn (FTO) và ứng dụng cho hệ chuyển động Robot Almega16. Nội dung chính bài báo là thiết kế bộ quan sát nhiễu với thời gian hữu hạn (FTO) sao cho việc quan sát các nhiễu ngoại của hệ thống chuyển động Robot Almega16 sẽ hội tụ về giá trị thực mong muốn với một khoảng thời gian hữu hạn, được thực hiện bằng cách là ước lượng các đại lượng nhiễu ngoại sau đó đưa vào bộ điều khiển Robot có sẵn. Ưu điểm khi ứng dụng bộ quan sát nhiễu FTO là có thể loại bỏ thành phần ma trận quán tính nghịch đảo trong phương trình động lực học. Kết quả đạt được, cho thấy hệ chuyển động Robot Almega16 đảm bảo sai số của các khớp quay nhanh chóng đạt tới không với thời gian quá độ nhỏ, làm cho hệ thống kín ổn định theo tiêu chuẩn Lyapunov.

Từ khóa: Robot Almega 16, bộ quan sát nhiễu với thời gian hữu hạn, tiêu chuẩn Lyapunov.

University of Economics - Technology for Industries

Email: vtha@uneti.edu.vn

Received: 16/4/2021

Revised: 20/5/2021

Accepted: 25/6/2021

1. INTRODUCTION

In the kinetic equation of industrial manipulator [26], there are always external noise components and internal noise. Especially the external noise components inside are unknown or not exactly known and these are the components that cause the movement of the hand

machine not to stick exactly to the given trajectory. To know the exact external noise components, it is necessary to incorporate a noise observation device (DOB) to estimate these disturbances. When applying the DOB noise monitor in the mechanical hand movement system, control can be based on the noise monitor [1-3], estimate and compensate the friction component [4,5], control force or torque. non-sensor torque [6-8], error diagnosis and isolation (FDI) [9-11]. The DOB turbulence monitor has been widely used in hand machine motion control for a variety of purposes. The basic idea of DOB is to use the motion state variables of the robot and the torque of the joints as input values and then estimate all the unknown internal and external torque. In [5], the Nonlinear Noise Observer (NDOB) was established to estimate the friction component so that accurate real friction component values can be known with fast time. The NDOB is done by choosing a certain nonlinear function. But the downside of the NDOB is that choosing such a nonlinear function is not straightforward. In [9], the use of the generalized momentum observer (GMO) has the advantage of not only avoiding acceleration calculations to reduce the effect of noise in site measurements, but also creating disturbance observations at superlative form. GMOs are able to realize FDI such as predicting random effects as well as saturation actuator error. The GMO Observer is easy to implement and has reliable results and the GMO has become a popular and widely used method in many hand-operated applications. However, the downside of GMOs is that the failure to return diagnostic results and slow response isolation (FDI) results in reduced sensitivity and response speed when the GMO is used in the case of collision detection. In [10] there was a solution for the GMO set, by treating the collision detection case as an extrinsic perturbation. Although many DOB observers have been developed and used for mechanical hand movement systems [5,9,10,13,14]. However, this DOB observer shows that the asymptotic convergence rate and the estimated bias of the perturbations will not converge quickly to zero. So for the conventional DOB convergence rate is best exponentially while the FTO can achieve a faster convergence rate with convergence in finite time. Given their finite time characteristics, a number of FTOs have been designed and applied to different systems with

versatile applications [15-20]. In this paper, a new DOB is shown. form is based on the requirement of fast and accurate estimation of robot disturbances. Based on the robot's dynamic model, the finite time control concept is used in the observer design. The resulting FTO can allow for estimation of the disturbance for a finite time, this ensures that the estimated error can disappear after a certain time. The proposed FTO also eliminates the need for acceleration calculation. Its finite-time convergence feature makes observing perturbations more accurate and fast. The structure of the paper is presented as follows: Part 1, problematic, Part 2 is the introduction of the Almega robot control object 16. Part 3 is detailed about robot dynamics and stability in time. finite time. Part 4 is an introduction to the FTO Observer. Part 5 is the application of the FTO controller to the Almega 16. Robot motion system. Part 6 is the conclusion.

2. OBJECT CONTROL

The Almega 16 robot is shown in Figure 1, as follows [25]. This is a vertical welding robot with fast, rhythmic and precise movement characteristics, including six-link axes, each one link axes is equipped with a permanent magnet synchronous servo motor and closed loop control. In the article using only three-link axes as the research object, specifically the main specifications of the three joints as follows.



Figure 1. Six-link Almega 16 arm

First joint: Rotation angle: $\pm 135^\circ$. Center tops from top to bottom: 28cm. Center line of axis I to the center of the cylinder: 35cm. Second joint: Rotation angle: $\pm 135^\circ$. The length between the center of the axis I and II is 65cm. Third joint: Angle of rotation: 90° and -45° . The length between the two centers of axis I and II is 47cm. The total volume of the Almega16 Robot: $V = 0.12035m^3$. Total weight of the robot: 250kg. The mass of joints is as follows: $m_0 = 100kg$, $m_1 = 67kg$, $m_2 = 52kg$, $m_3 = 16kg$, $m_4 = 10kg$, $m_5 = 4kg$, $m_6 = 1kg$.

The motion system Almega16 Robot is a nonlinear system that has constant model parameters and is interfering with the channel between the component motion axes. According to the literature as follows [26], the first three joints have fully integrated the dynamics of the freedom arm. The motor connected to the joint is usually a

planetary gear and Small air gap. It is influenced by friction such as static friction, friction, viscous friction and so on. Therefore, the first three joints are the basic chain that ensures movement in 3D (X, Y, Z) space. The basis for the study of the next steps in robot manipulator motion systems. The problem with the controller is that: should design the quality control ensures precise orbit grip that does not depend on the parameters of the model uncertainty and the impact on channel mix between match-axis error between joint angles and the angle joints actually put a small ($< 0.1\%$).

3. PRELIMINARIES

3.1. Robot Dynamic Model

The dynamic of an n-link rigid manipular, [1-4, 6] can be written as

$$\tau + \tau_d = M(q)\ddot{q} + C(q, \dot{q})\dot{q} + G(q) + \tau_f \tag{1}$$

Where q is the $n \times 1$ joint variable vector, τ is a $n \times 1$ generalized torque vector $M(q)$ is the $n \times n$ inertia matrix, $H(q, \dot{q})$ is the $n \times 1$ Coriolis/centripetal vector, $G(q)$ is the $n \times 1$ gravity vector. $\tau_d \in R^n$ denotes the lumped friction effect from both the motor and link sides and are always described with the following Coulomb-viscous model, namely

$$\tau_f = F_c \text{sgn}(\dot{q}) + F_v \dot{q} \tag{2}$$

with $F_c = \text{diag}\{F_{c1}, \dots, F_{cn}\}$, $F_v = \text{diag}\{F_{v1}, \dots, F_{vn}\}$, F_{ci}, F_{vi} ($1 \leq i \leq n$) are the Coulomb and viscous friction coefficients for the i th joint. Such a friction model could capture most dynamic property of the friction in a rigid joint. The equivalent motor torque at the link side through a reduced amplification is denoted as $\tau \in R^n$, $\tau_d \in R^n$ is the internal/external disturbances which could be an external force, unmodeled or uncertain robot dynamics. The exact meaning of τ_d decides on the specific application. The observed disturbance for a manipulator can be further utilized in FDI and disturbance rejection control. For example, τ_d is deemed as the physical impact with the environment for collision detection scenario and, thus, τ_d can indicate the occurrence of the collision. The robot dynamics model in Equation (1) has the following property.

In which 1: The matrix $\dot{M}(q) - 2C(q, \dot{q})$ is skew-symmetry [21], and it follows that

$$\dot{M}(q) = C(q, \dot{q}) + C^T(q, \dot{q}) \tag{3}$$

3.2. Disturbance Observer GMO

In order to estimate the external beeb-type noise components for hand-operated systems, there are many different monitors. One of the most commonly used observers is the observed (GMO) observed in Reference [9]. Combined with the generalized momentum p , in Equation (1) could be rewritten to

$$\dot{p} = \tau + C^T(q, \dot{q})\dot{q} - G(q) + \tau_d \tag{4}$$

The GMO component p is estimated as follows:

$$\hat{\mathbf{p}} = \boldsymbol{\tau} + \mathbf{C}^T(\mathbf{q}, \dot{\mathbf{q}})\dot{\mathbf{q}} - \mathbf{G}(\mathbf{q}) + \hat{\boldsymbol{\tau}}_d \quad (5)$$

$$\hat{\boldsymbol{\tau}}_d = \mathbf{K}_0(\mathbf{p} - \hat{\mathbf{p}}) \quad (6)$$

where (\cdot) denotes the estimated value and $\mathbf{K}_0 = \text{diag}\{k_{0i}\} > 0$. So the estimate of the external disturbance is given is:

$$\hat{\boldsymbol{\tau}}_d = \mathbf{K}_0 \int (\boldsymbol{\tau} + \mathbf{C}^T(\mathbf{q}, \dot{\mathbf{q}})\dot{\mathbf{q}} - \mathbf{G}(\mathbf{q}) + \hat{\boldsymbol{\tau}}_d) dt \quad (7)$$

From equations (5) and (6), are determined:

$$\hat{\boldsymbol{\tau}}_d = \mathbf{K}_0(\boldsymbol{\tau}_d - \hat{\boldsymbol{\tau}}_d) \quad (8)$$

or convert to a Laplace image which will be written in the following format:

$$\hat{\boldsymbol{\tau}}_d = \frac{\mathbf{K}_0}{s + \mathbf{K}_0} \boldsymbol{\tau}_d \quad (9)$$

According to reference [9] shows that the component $\hat{\boldsymbol{\tau}}_d$ is a first order inertial function $\boldsymbol{\tau}_d$. So the external perturbation estimation $\hat{\boldsymbol{\tau}}_d$ component of the GMO will converge exponentially and depend on the observation matrix \mathbf{K}_0 . Therefore, the GMO observer always has an estimated bias in the outer perturbations.

3.3. Consider steady state in finite time

Consider the following nonlinear system

$$\dot{\mathbf{x}} = \mathbf{f}(\mathbf{x}), \mathbf{x} \in \mathbf{R}^n, \mathbf{f}(\mathbf{0}) = \mathbf{0} \quad (10)$$

where \mathbf{f} satisfies the locally Lipschitz continuous condition. Some basic knowledge about finite time homogeneity and stability (FTS) in the document [22,23].

4. FINITE-TIME OBSERVER OF ROBOTIC DISTURBANCE

The main content of this paper is to design a finite time observer so that the observation of the noise τ_d can converge to its true value in a finite time. In this section 4 will be presented on the content of constructing the FTO observer to estimate the external perturbations. After the estimation is complete, the state variables estimate the external perturbations to the existing control system such as the PID controller,.... When the FTO Observer is connected, the calculation and elimination will be reduced. remove the inverse inertial matrix in the kinetic equation.

4.1. Finite-Time Observer Design

From Equation (1), the acceleration $\ddot{\mathbf{q}}$ can be written as

$$\ddot{\mathbf{q}} = \mathbf{M}^{-1}(\mathbf{q})\boldsymbol{\tau}_d + \mathbf{M}^{-1}(\mathbf{q})(\boldsymbol{\tau} - \mathbf{C}(\mathbf{q}, \dot{\mathbf{q}})\dot{\mathbf{q}} - \mathbf{G}(\mathbf{q}) - \boldsymbol{\tau}_f) \quad (11)$$

Put: $\boldsymbol{\tau}_a = \boldsymbol{\tau} - \mathbf{C}(\mathbf{q}, \dot{\mathbf{q}})\dot{\mathbf{q}} - \mathbf{G}(\mathbf{q}) - \boldsymbol{\tau}_f$, then (11) is rewritten as follows as:

$$\ddot{\mathbf{q}} = \mathbf{M}^{-1}(\mathbf{q})\boldsymbol{\tau}_d + \mathbf{M}^{-1}(\mathbf{q})\boldsymbol{\tau}_a \quad (12)$$

where $\mathbf{M}^{-1}(\mathbf{q})\boldsymbol{\tau}_d$ is treated as the system disturbances with $\mathbf{M}^{-1}(\mathbf{q})\boldsymbol{\tau}_a$ the system input. According to reference [20], the FTO monitor for manipulators is specifically designed as follows:

$$\dot{\mathbf{z}}_{b1} = \mathbf{z}_{b2} + \mathbf{K}_1 \lfloor \mathbf{e}_b \rfloor^{\alpha_1} \quad (13)$$

$$\dot{\mathbf{z}}_{b2} = \mathbf{z}_{b3} + \mathbf{M}^{-1}(\mathbf{q})\boldsymbol{\tau}_a + \mathbf{K}_2 \lfloor \mathbf{e}_b \rfloor^{\alpha_2} \quad (14)$$

$$\dot{\mathbf{z}}_{b3} = \mathbf{K}_3 \lfloor \mathbf{e}_b \rfloor^{\alpha_3} \quad (15)$$

Where $\mathbf{z}_{b1} = \dot{\mathbf{q}}, \mathbf{z}_{b2} = \ddot{\mathbf{q}}, \mathbf{z}_{b3} = \mathbf{M}^{-1}(\mathbf{q})\boldsymbol{\tau}_d$ and $\mathbf{e}_b = \mathbf{q} - \hat{\mathbf{q}}, \mathbf{K}_1, \mathbf{K}_2, \mathbf{K}_3 \in \mathbf{R}^{n \times n}$ are diagonal gain matrices. Moreover, the corresponding powers are selected as $\alpha_1 = \alpha, \alpha_2 = 2\alpha - 1, \alpha_3 = 3\alpha - 1$ and $\frac{2}{3} < \alpha < 1$. The operator $\lfloor \cdot \rfloor^\alpha$ is denoted as

$$\lfloor \mathbf{x} \rfloor^\alpha = |\mathbf{x}|^\alpha \text{sgn}(\mathbf{x}), \mathbf{x} \in \mathbf{R}^n \text{ and } \alpha > 0 \quad (16)$$

Consequently, the disturbance observation $\hat{\boldsymbol{\tau}}_d$ is computed as

$$\hat{\boldsymbol{\tau}}_d = \mathbf{M}(\mathbf{q})\mathbf{z}_{b3} \quad (17)$$

From (17) shows, the proposed FTO is a ternary system that can simultaneously estimate the joint velocity and the external perturbation component. It shows that the joint velocity can be obtained instantly from the robot control system. From the formula (13) - (15), it is possible to downgrade the observational equation for external disturbance state variables leading to a reduction in the computational heavy process. Therefore, the downgrade FTO is determined as follows:

$$\dot{\mathbf{z}}_{r1} = \mathbf{z}_{r2} + \mathbf{M}^{-1}(\mathbf{q})\boldsymbol{\tau}_a + \mathbf{K}_1 \lfloor \mathbf{e}_r \rfloor^{\alpha_1} \quad (18)$$

$$\dot{\mathbf{z}}_{r2} = \mathbf{K}_2 \lfloor \mathbf{e}_r \rfloor^{\alpha_2} \quad (19)$$

Where $\mathbf{z}_{b1} = \dot{\mathbf{q}}, \mathbf{z}_{b2} = \mathbf{M}^{-1}(\mathbf{q})\boldsymbol{\tau}_d$ and $\mathbf{e}_b = \mathbf{q} - \hat{\mathbf{q}}, \alpha_1 = \alpha, \alpha_2 = 2\alpha - 1, \frac{1}{2} < \alpha < 1$. From formula (19), we determine the formula to calculate the estimate of the external disturbance is determined as follows:

$$\hat{\boldsymbol{\tau}}_d = \mathbf{M}(\mathbf{q})\mathbf{z}_{r2} \quad (20)$$

The decremented FOT observer will estimate the perturbed state variables faster than the original unremarked design. And from formula (12) shows that still exists the inverse matrix component of $\mathbf{M}(\mathbf{q})$. To remove the inverse inertial matrix component of $\mathbf{M}(\mathbf{q})$, it is necessary to rearrange the original system from equation (12) into a transformed equation with different state variables. Multiplying both sides of Equation (12) by $\mathbf{M}(\mathbf{q})$ yields the following:

$$\mathbf{M}(\mathbf{q})\ddot{\mathbf{q}} = \boldsymbol{\tau}_a + \boldsymbol{\tau}_d \quad (21)$$

Additionally, the left side of Equation (21) could be altered using the generalized momentum \mathbf{p} , namely

$$\dot{\mathbf{p}} - \dot{\mathbf{M}}(\mathbf{q})\dot{\mathbf{q}} = \boldsymbol{\tau}_a + \boldsymbol{\tau}_d \quad (22)$$

Reorganizing Equation (22) and employing Property 1, the derivative of the generalized momentum \mathbf{p} is rewritten as

$$\dot{\mathbf{p}} = \boldsymbol{\tau}_d + \boldsymbol{\tau}_p \quad (23)$$

Where $\tau_p = \dot{M}(q)\dot{q} + \tau_a = \tau + \varphi(q, \dot{q}) = C^T(q, \dot{q})\dot{q} - G(q) - \tau_f$. The system should observe that the externally implemented perturbation variables have been altered and have different state variables. A set of FTOs reduced from tertiary to quadratic is replaced as follows:

$$\dot{z}_{m1} = z_{m2} + \tau_p + K_1 [e_m]^{\alpha_1} \tag{24}$$

$$\dot{z}_{m2} = K_2 [e_m]^{\alpha_2} \tag{25}$$

where $z_{m1} = \hat{q}$, $z_{m2} = \hat{\tau}_d$ and $e_m = q - \hat{q}$.

The control structure diagram with FTO is shown in figure 2.

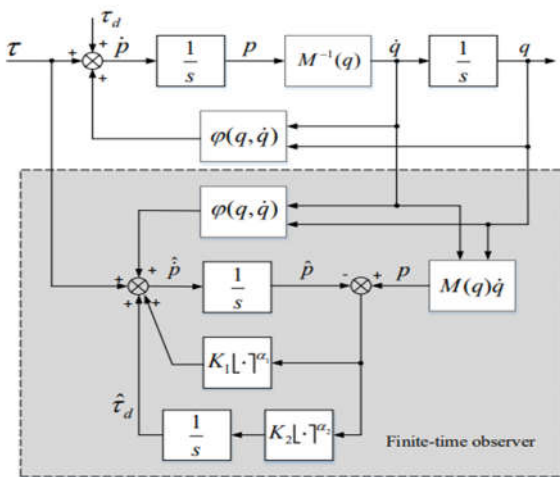


Figure 2. The control structure diagram with FTO of robotic disturbance finite-time observer

The obtained FTO given in Equations (24) and (25) is structurally similar to the GMO defined in Equations (5) and (6) as both observer shares the same system states and input. The obtained FTO observer is represented in Equations (26) and (27) and has an estimation structure of external perturbation variables similar to that identified in Equations (5) and (6), since both of these observers use system state variables and as input signals.

4.2. Consider the stability and convergence of the FTO

The observation errors are given as:

$$\dot{e}_p = e_d - K_1 [e_p]^{\alpha_1} \tag{26}$$

$$\dot{e}_d = -K_2 [e_p]^{\alpha_2} \tag{27}$$

Where $e_p = p - \hat{p}$, $e_d = \tau_d - \hat{\tau}_d$, $e = [e_p, e_d]$.

Using Lyapunov standard to prove the stability of the FTO is proposed as follows;

Given a positive defined function, (28):

$$V = \sum_{i=1}^n k_{2i} \int_0^{e_{pi}} [\tau]^{\alpha_2} dt + \frac{e_d^T e_d}{2} = \sum_{i=1}^n \frac{k_{2i}}{\alpha_2 + 1} e_{pi}^{\alpha_2 + 1} + \frac{e_d^T e_d}{2} \tag{28}$$

where k_{2i} is the i th diagonal element of K_2 . Then its derivative is

$$\begin{aligned} \dot{V} &= \frac{\partial V}{\partial e^T} \dot{e} \\ &= \sum_{i=1}^n k_{2i} [e_{pi}]^{\alpha_2} (e_{di} - K_1) [e_{pi}]^{\alpha_1} - e_d^T K_2 [e_{pi}]^{\alpha_2} \\ &= e_d^T K_2 [e_{pi}]^{\alpha_2} - \sum_{i=1}^n k_{1i} k_{2i} [e_{pi}]^{\alpha_1 + \alpha_2} - e_d^T K_2 [e_{pi}]^{\alpha_2} \\ &= -\sum_{i=1}^n k_{1i} k_{2i} [e_{pi}]^{\alpha_1 + \alpha_2} \leq 0 \end{aligned} \tag{29}$$

Where k_{1i} is a positive defined diagonal element of K_1 and such that $e_p = e_d = 0$. Apply to LaShalle's theorem, to ensure that the asymptotic convergence of the deviation e to 0 is guaranteed. The next content of the paper will present about demonstrating the observer's finite convergence of time. According to Definition 2 [27], Equations (28) and (29) are orderly homogeneous with respect to weight. Hence, consider equations (28) and (29) that have a negative identity. From Theorem 1, [27], the error system is the global FTO. In other words, the estimated deviations of the turbulent state variables will disappear for a finite time. From that it can be concluded, the proposed downgrade FTO is stable and with convergent efficiency in finite time...

5. SIMULATION RESULTS

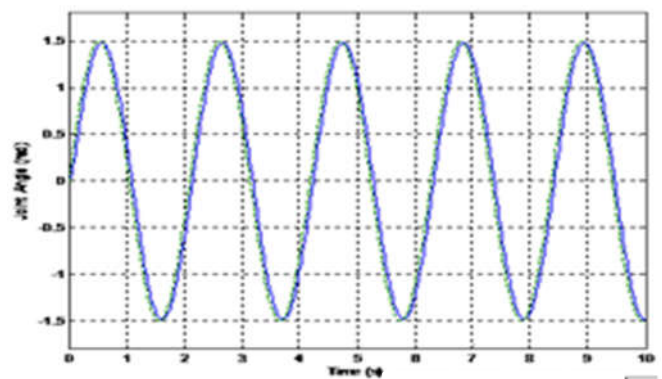
Afer building up the algorithms and control programs, we will proceed to run the simulation program to test computer program. The FTO was Simulink with Table 1.

Table 1. The Parameter of FTO

Symbol	The parameter	The Parameter value of the joint axis
q_d	Desired joint position	$q_{d1} = q_{d2} = q_{d3} = \text{sint}$
K_1	Scalar	$K_1 = [200, 200, 200]$
K_2	Constant	$K_2 = [10000, 10000, 10000]$
α	Power coefficient	$\alpha = 1$
τ_d	Disturbance	sint

After simulation we have results position and position tracking error is depicted Figure 3÷ 7.

* Desired joint position is $\text{sin}(t)$



Joint 1

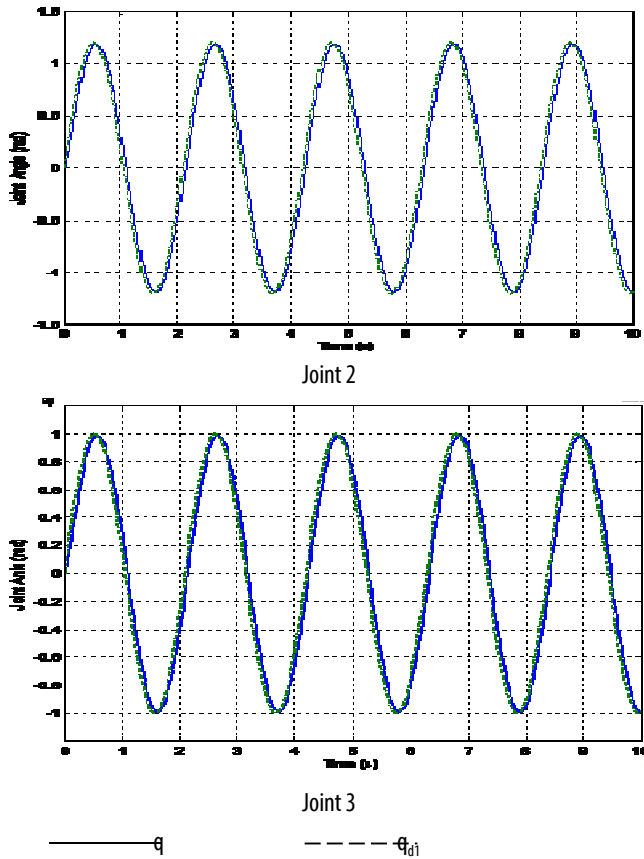


Figure 3. Performing deviation between the angles q set and q real

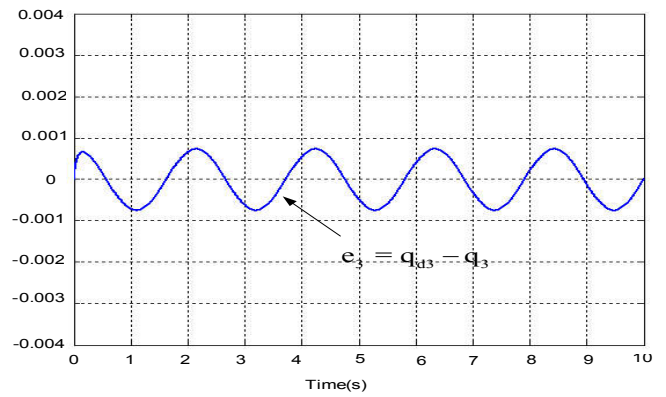
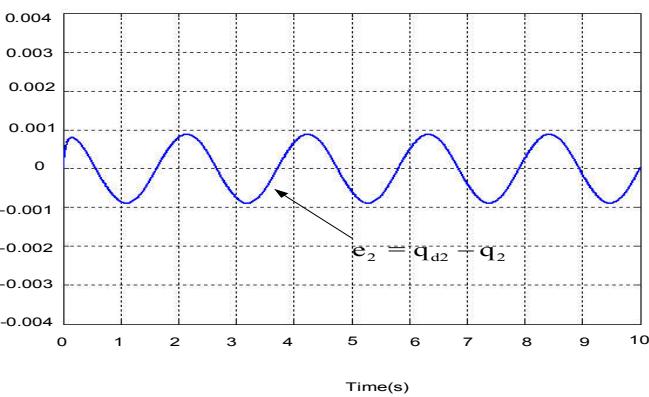
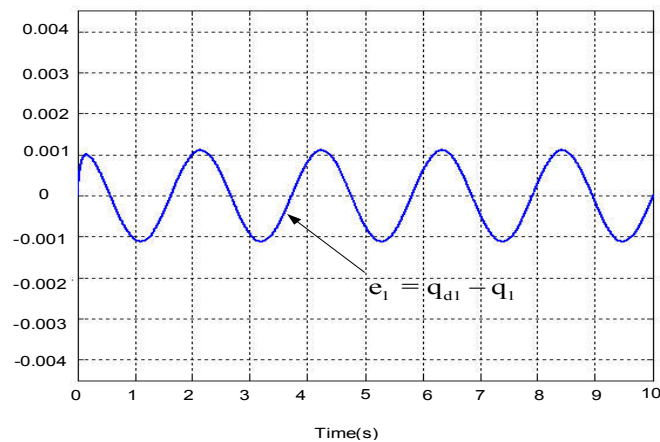


Figure 4. Express the response between the set angles q and real q

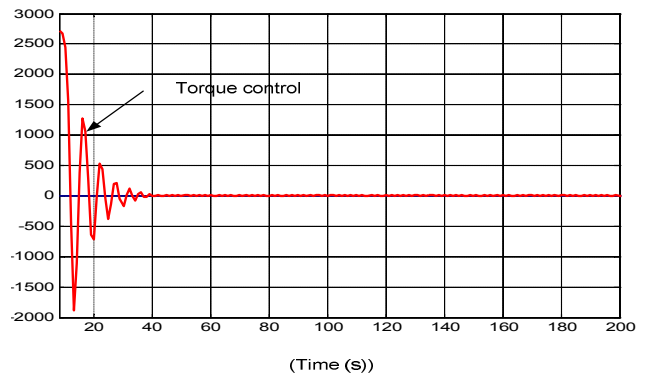


Figure 5. Express the control moments of the controller joints

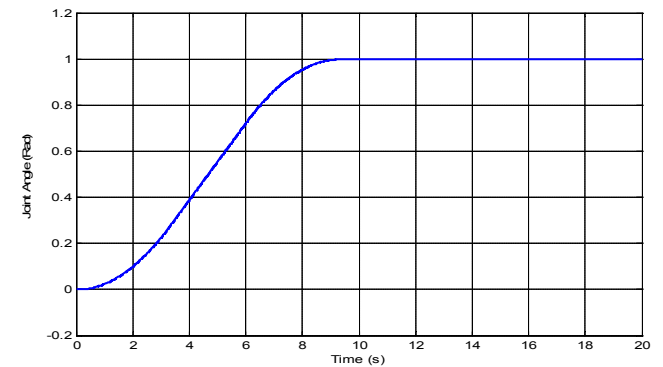


Figure 6. Performing the response of the actual joint position and the actual joint position

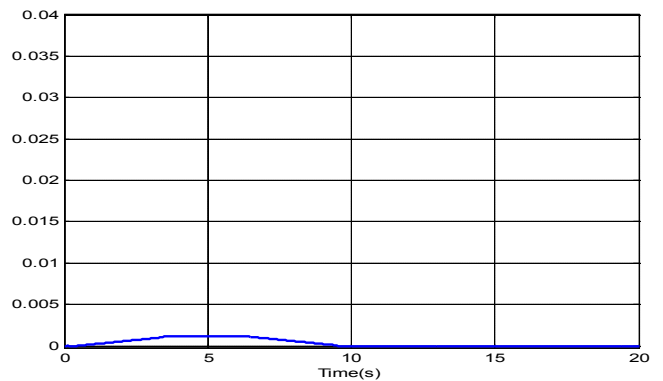


Figure 7. The deviation response controls the actual joint position and estimated joint position

Comment: The simulation results of the real state and the above estimate prove that the synthesized FTO observer is correct, showing that the joints of the Almega 16 robot are good with small setting time, less oscillation, over-adjustment.

6. CONCLUSION

The order reduction FTO has omitted acceleration and inverse matrix matrix, resulting in the FTO making the estimation deviations converge to 0 in a finite time. Although FTO has a more complex formula and thus the calculation time increases slightly compared to other observers. The theory and simulation results show that using the FTO observatory to estimate the perturbation components outside the Almega 16 robot motion system has ensured the real joint position closely follows the estimated joint position and ensures the actual matching position is closely related to the matching position with small error.

REFERENCES

- [1]. Pi Y., Wang X., 2010. *Observer-based cascade control of a 6-DOF parallel hydraulic manipulator in joint space coordinate*. *Mechatronics*, 20, 648–655.
- [2]. Sahabi M.E., Li G., Wang X., Li S., 2016. *Disturbance Compensation Based Finite-Time Tracking Control of Rigid Manipulator*. *Math. Probl. Eng.* 2016, 2034795.
- [3]. Chen W.H., Yang J., Guo L., Li S., 2016. *Disturbance-observer-based control and related methods-An overview*. *IEEE Trans. Ind. Electron.*, 63, 1083–1095.
- [4]. Bona B., Indri M., 2005. *Friction compensation in robotics: An overview*. In *Proceedings of the 44th IEEE Conference on Decision and Control*, Seville, Spain, pp. 4360–4367.
- [5]. Chen W.H., Ballance D.J., Gawthrop P.J., O'Reilly J., 2000. *A nonlinear disturbance observer for robotic manipulators*. *IEEE Trans. Ind. Electron.*, 47, 932–938.
- [6]. Magrini E., Flacco F., De Luca A., 2015. *Control of generalized contact motion and force in physical human-robot interaction*. In *Proceedings of the 2015 IEEE International Conference on Robotics and Automation (ICRA)*, Seattle, WA, USA, pp. 2298–2304.
- [7]. Magrini E., De Luca A., 2016. *Hybrid force/velocity control for physical human-robot collaboration tasks*. In *Proceedings of the 2016 IEEE/RSJ International Conference on Intelligent Robots and Systems (IROS)*, Daejeon, Korea, pp. 857–863.
- [8]. Gaz C., Magrini E., De Luca A., 2018. *A model-based residual approach for human-robot collaboration during manual polishing operations*. *Mechatronics* 55, 234–247.
- [9]. De Luca A., Mattone R., 2003. *Actuator failure detection and isolation using generalized momenta*. In *Proceedings of the IEEE International Conference on Robotics and Automation*, Taipei, Taiwan, Volume 1, pp. 634–639.
- [10]. Ren T., Dong Y., Wu D., Chen K., 2018. *Collision detection and identification for robot manipulators based on extended state observer*. *Control Eng. Pract.*, 79, 144–153.
- [11]. Haddadin S., De Luca A., Albu-Schäffer A., 2017. *Robot collisions: A survey on detection, isolation, and identification*. *IEEE Trans. Robot.*, 33, 1292–1312.
- [12]. Cho C.N., Kim J.H., Kim Y.L., Song J.B., Kyung J.H., 2012. *Collision detection algorithm to distinguish between intended contact and unexpected collision*. *Adv. Robot.*, 26, 1825–1840.
- [13]. Mohammadi A., Tavakoli M., Marquez H.J., Hashemzadeh F., 2013. *Nonlinear disturbance observer design for robotic manipulators*. *Control Eng. Pract.*, 21, 253–267.
- [14]. Nikoobin A., Haghghi R., 2009. *Lyapunov-based nonlinear disturbance observer for serial n-link robot manipulators*. *J. Intell. Robot. Syst.*, 55, 135–153.
- [15]. Menard T., Moulay E., Perruquetti W., 2010. *A global high-gain finite-time observer*. *IEEE Trans. Autom. Control*, 55, 1500–1506.
- [16]. Lopez-Ramirez F., Polyakov A., Efimov D., Perruquetti W., 2018. *Finite-time and fixed-time observer design: Implicit Lyapunov function approach*. *Automatica*, 87, 52–60.
- [17]. Menard T., Moulay E., Perruquetti W., 2017. *Fixed-time observer with simple gains for uncertain systems*. *Automatica*, 81, 438–446.
- [18]. Shen Y., Xia X., 2008. *Semi-global finite-time observers for nonlinear systems*. *Automatica*, 44, 3152–3156.
- [19]. Shtessel Y.B., Shkolnikov I.A., Levant A., 2007. *Smooth second-order sliding modes: Missile guidance application*. *Automatica*, 43, 1470–1476.
- [20]. Perruquetti W., Floquet T., Moulay E., 2008. *Finite-time observers: Application to secure communication*. *IEEE Trans. Autom. Control*, 53, 356–360.
- [21]. Siciliano B., Sciavicco L., Villani L., Oriolo G., 2010. *Robotics: Modelling, Planning and Control*. Springer Science & Business Media: Berlin/Heidelberg, Germany.
- [22]. Bhat S.P., Bernstein D.S., 2000. *Finite-time stability of continuous autonomous systems*. *SIAM J. Control Optim.*, 38, 751–766.
- [23]. Bhat S.P., Bernstein D.S., 2005. *Geometric homogeneity with applications to finite-time stability*. *Math. Control. Signals Syst.*, 17, 101–127.
- [24]. Bacciotti A., Rosier L., 2006. *Liapunov Functions and Stability in Control Theory*. Springer Science & Business Media: Berlin/Heidelberg, Germany.
- [25]. Ha V. T., 2012. *Some control solutions aim to improve the quality of industrial hand motions*. Ph.D. thesis, Hanoi University of Science and Technology.
- [26]. Neil M., Frank L.L., 2004. *Robot Manipulator Control Theory and Practice*. Marcel Dekker.
- [27]. Pengfei Cao, Yahui Gan, Xianzhong Dai, 2019. *Finite-Time Disturbance Observer for Robotic Manipulators*. *Sensors (Basel)*, 19(8):1943. doi: 10.3390/s19081943.

THÔNG TIN TÁC GIẢ

Võ Thu Hà

Trường Đại học Kinh tế - Kỹ thuật Công nghiệp